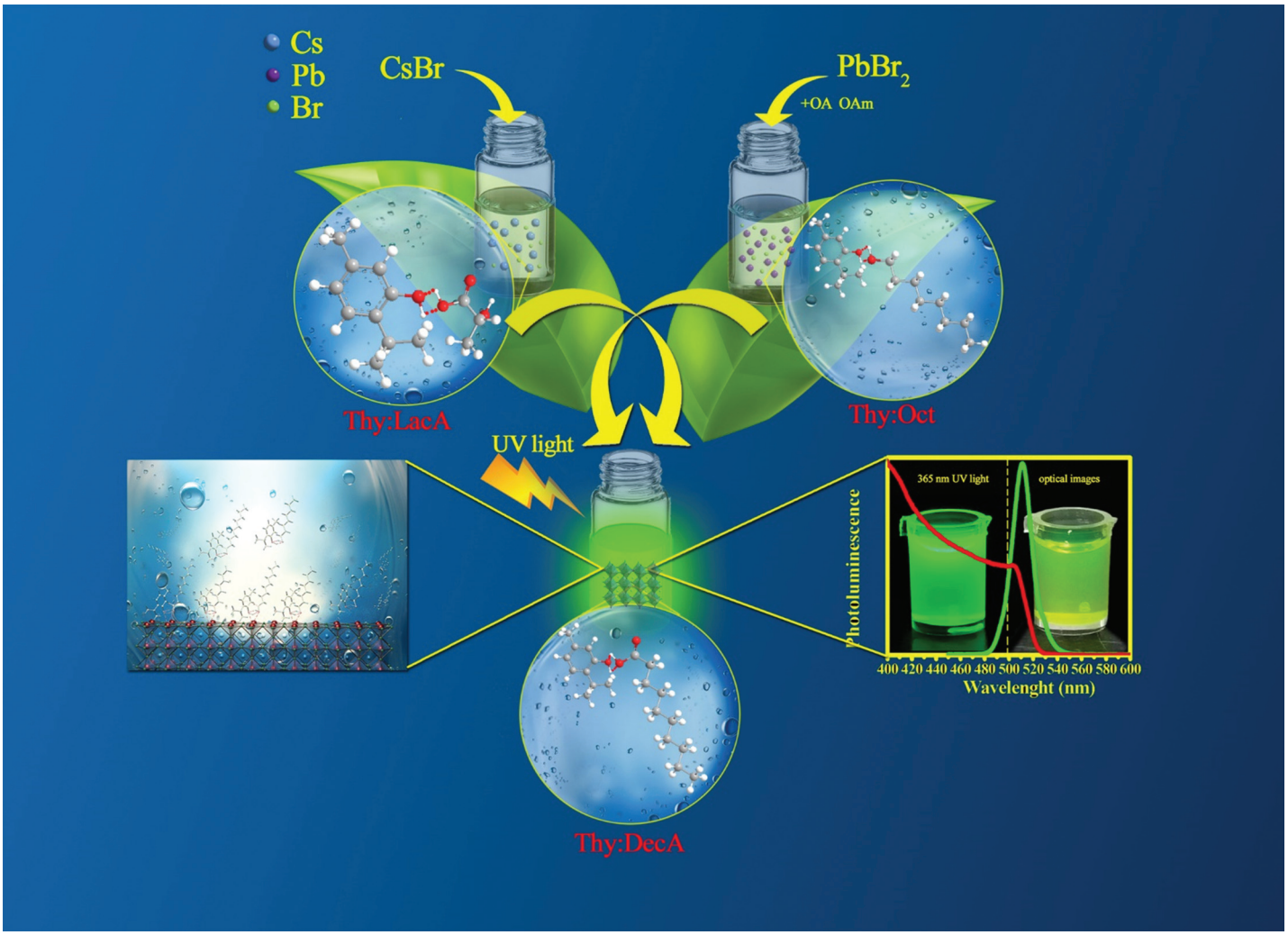

Showcasing research from Prof. Mao-Sheng Zhang's group at Fujian Province University Key Laboratory of Analytical Science, Minnan Normal University, Zhangzhou, China.

Green synthesis of highly stable $CsPbBr_3$ perovskite nanocrystals using natural deep eutectic solvents as solvents and surface ligands

A facile, rapid and toxic organic solvent-free synthesis strategy of $CsPbBr_3$ PNCs was developed for the first time *via* the ligand-assisted reprecipitation (LARP) method using natural deep eutectic solvents (NADESs) as solvents and surface ligands. The as-synthesized $CsPbBr_3$ NCs exhibited high photoluminescence quantum yield, narrow full width at half-maximum and high stability. This work provides a new strategy for green synthesis of PNCs, which promises feasibility for industrial large-scale synthesis of PNCs.

As featured in:

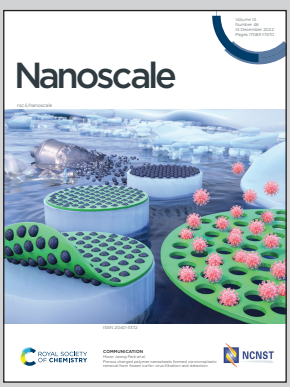

See Maosheng Zhang *et al.*, *Nanoscale*, 2022, **14**, 17222.

ROYAL SOCIETY OF CHEMISTRY

rsc.li/nanoscale

Registered charity number: 207890

Nanoscale

PAPER

View Article Online
View Journal | View Issue

Check for updates

Cite this: *Nanoscale*, 2022, **14**, 17222

Green synthesis of highly stable $CsPbBr_3$ perovskite nanocrystals using natural deep eutectic solvents as solvents and surface ligands†

Heng Lu,[a] Xiaohong Tan,[a] Guobin Huang,[c] Shaoru Wu,[a] Yanmei Zhou,[a] Junying Zhang,[a] Qiaowen Zheng,[a] Tianju Chen,[a] Feiming Li,[a,b] Zhixiong Cai,[a,b] Jingbin Zeng[d] and Maosheng Zhang *[a,b]

Received 28th July 2022,
Accepted 10th October 2022

DOI: 10.1039/d2nr04173a

rsc.li/nanoscale

Perovskite nanocrystals (PNCs) have attracted widespread attention as promising materials for the optoelectronic field due to their remarkable photophysical properties and structural tunability. However, their poor stability and the use of toxic organic solvents in the preparation process have severely restricted their practical applications. Herein, a facile, rapid and toxic organic solvent-free synthesis strategy of $CsPbBr_3$ PNCs was developed for the first time *via* the ligand-assisted reprecipitation (LARP) method using natural deep eutectic solvents (NADESs) as solvents and surface ligands. In this method, the NADESs not only functioned as solvents for green synthesis, but also served simultaneously as surface ligands of $CsPbBr_3$ PNCs to significantly improve their optical properties and stability. The as-synthesized $CsPbBr_3$ PNCs exhibited high photoluminescence quantum yield (PLQY, ~96.8%), narrow full width at half-maximum (FWHM, ~18.8 nm) and a high stability that retained 82.9% of PL intensity after 70 days. This work provides a new strategy for the green synthesis of PNCs, which promises feasibility for the industrial large-scale synthesis of high-quality PNCs.

Published on 11 Oktoba 2022. Downloaded on 26/07/2025 17:39:36.

Introduction

In recent years, perovskite nanocrystals (PNCs) have received much attention because of their excellent optoelectronic properties, such as narrow full width at half-maximum (FWHM), high photoluminescence quantum yield (PLQY), low exciton binding energy, tunable band gap, and low defect density.[1–3] They show great potential for application in the fields of light-emitting diodes (LED),[4,5] solar cells,[6–8] lasers[9] and photocatalysis.[10–12] Currently, the most common synthesis methods for PNCs are the hot-injection method[13] and the ligand-assisted reprecipitation (LARP) method.[14,15] In the LARP method, PNCs are obtained through the regulation of volume and concentration of solvents and precursors. Precursors are firstly dissolved in good solvents, such as dimethyl sulfoxide (DMSO) and dimethylformamide (DMF), and then transferred into poor solvents (antisolvents), such as toluene and *n*-octane, to form a supersaturated solution and precipitate the crystals under the assistance of ligands, such as oleic acid (OA) and oleylamine (OAm). This method is promising due to its ease of operation, low equipment requirement and mild operational temperatures. However, there are two disadvantages of the LARP method. On the one hand, a large amount of toxic organic solvents is inevitably used, which significantly limits their applications. On the other hand, the proton exchange between OA and OAm may induce the ligands to be easily lost from the surface of PNCs during the purification process or storage period, resulting in poor stability of PNCs.

Recently, great efforts have been devoted to developing effective ways to solve the above problems. Li[16] *et al.* developed a novel low-toxicity antisolvent synthesis (LTAS) process based on tetraethyl orthosilicate (TEOS) to obtain monodispersed and luminescent all-inorganic PNCs. Wang's[17] group proposed a facile method to synthesize green $CsPbBr_3$ PNCs using the ionic liquid (IL) 1-butyl-3-methylimidazolium bromide ([Bmim]Br). Luo[18] *et al.* recently reported the synthesis of blue-emission $CsPbBr_3$ PNCs with the assistance of hydrophobic ILs. However, ILs have some disadvantages, such as complex preparation processes, high cost and poor biocompatibility.[19,20] In addition, Tan[21] *et al.* proposed a novel strategy using octylphosphonic acid (OPA) as the capping

[a]*College of Chemistry, Chemical Engineering and Environment, Minnan Normal University, Zhangzhou 363000, China. E-mail: zms0557@mnnu.edu.cn*
[b]*Fujian Province Key Laboratory of Modern Analytical Science and Separation Technology, Minnan Normal University, Zhangzhou 363000, China*
[c]*Institute of Food Safety and Environment Monitoring, Fuzhou University, Fuzhou 350108, China*
[d]*College of Science, China University of Petroleum (East China), Qingdao 266580, China*

† Electronic supplementary information (ESI) available. See DOI: https://doi.org/10.1039/d2nr04173a

This journal is © The Royal Society of Chemistry 2022

Published on 11 Oktoba 2022. Downloaded on 26/07/2025 17:39:36.

ligand to solve the problem of ligands loss and improve the stability of $CsPbX_3$ PNCs. Mishra[22] *et al.* reported bromopropane as a novel bromine precursor for the completely amine-free colloidal synthesis of $CsPbBr_3$ PNCs. Research on the direction of amine-free synthesis emerges in an endless stream.[23–25]

Deep eutectic solvents (DESs), introduced by Abbott[26] *et al.* in 2003, have been regarded as a new class of green solvents. DESs are low-eutectic mixtures of compounds composed of a hydrogen bond donor (HBA) and a hydrogen bond acceptor (HBD).[27] They possess not only similar favorable properties to ILs, but also the advantage of being easy to prepare, cost-effective, and biodegradable.[28,29] Among them, natural deep eutectic solvents (NADESs), composed of natural compounds such as carboxylic acids, sugars, alcohols, amines and amino acids, have attracted more attention because they fully meet the green chemistry principles.[30] As the most promising alternative to toxic organic solvents, NADESs have been applied successfully in the fields of catalysis,[31,32] extraction,[33,34] electrochemistry[35,36] and organic synthesis.[37,38] Furthermore, the –COOH, –OH, and $–NH_2$ groups in these natural compounds can coordinate with metal ions, which provides feasibility for using NADESs as ligands. To the best of our knowledge, NADESs used simultaneously as solvents and surface ligands in the synthesis of PNCs have not been reported so far.

Herein, a facile, rapid and toxic organic solvent-free synthesis strategy for $CsPbBr_3$ PNCs was developed for the first time *via* the ligand-assisted reprecipitation (LARP) method using NADESs as solvents and surface ligands. First, NADESs, consisting of thymol as the HBA and L-lactic acid (Thy : LacA) and *n*-octanol (Thy : Oct) as the HBD, were used as good solvents, and a NADES consisting of thymol as the HBA and decanoic acid (Thy : DecA) as the HBD was used as antisolvent for the green synthesis of NADES-$CsPbBr_3$ PNCs. Moreover, the –COOH and –OH groups in Thy : Oct and Thy : DecA can polychelate with Pb^{2+} and provide a strong interaction with $CsPbBr_3$ PNCs. Thereby, Thy : Oct and Thy : DecA can also act as surface ligands to significantly enhance the optical properties and stability of $CsPbBr_3$ PNCs. This facile, rapid and green synthesis method of PNCs will provide a new avenue for their sustainable industrial production in various fields.

Experimental

Reagents and solutions

DL-Menthol ($C_{10}H_{20}O$, 98%), thymol ($C_{10}H_{14}O$, 98%), L-lactic acid ($C_3H_6O_3$, 90%), *n*-octanoic acid ($C_8H_{16}O_2$, 99%), decanoic acid ($C_{10}H_{20}O_2$, 99%), lauric acid ($C_{12}H_{24}O_2$, 98%), oleic acid ($C_{18}H_{34}O_2$, AR), ethanol (C_2H_6O, 99%), *n*-butanol ($C_4H_{10}O$, 99%), *n*-hexanol ($C_6H_{14}O$, 99%), *n*-octanol ($C_8H_{18}O$, 99%), and cesium bromide (CsBr, 99.5%) were obtained from Aladdin Industrial Co. Ltd (Shanghai, China). *n*-Decanol ($C_{10}H_{22}O$, 98%), lead(II) bromide ($PbBr_2$, 99%), and oleylamine ($C1_8H_{37}N$, 80–90%) were purchased from Macklin Biochemical Technology Co. Ltd. (Shanghai, China). All reagents and solutions were used as received without further purification.

Apparatus

Fourier transform infrared (FTIR) spectra (NICOLET iS 10) and ^{1}H NMR (Avance 500 MHz; Bruker) were applied to determine the formation of NADESs. The phase of the NADES-$CsPbBr_3$ PNCs was identified *via* an X-ray diffractometer (XRD, Rigaku Ultima IV). Ultraviolet–visible (UV-vis) absorption spectra were tested using a UV-vis spectrophotometer (Specord plus 200). Photoluminescence (PL) emission spectra were recorded using a spectrometer (Techcomp FL970 Plus). NADES-$CsPbBr_3$ PNCs were characterized using luminescence decay curves and photoluminescence quantum yields (PLQY; FLS980, Edinburgh) under excitation at 365 nm. Transmission electron microscopy (TEM) images and high-resolution TEM images were taken on a JEM-2100.

Preparation of NADESs

In this study, different NADESs were prepared by the following steps. Firstly, the [HBA : HBD] of all NADESs was mixed at a molar ratio of 1 : 1, and using DL-menthol and thymol as the HBA, combined with eight different HBDs comprising L-lactic acid, *n*-octanoic acid, decanoic acid, lauric acid, ethanol, *n*-butanol, *n*-hexanol and *n*-octanol. Secondly, the mixture was heated and stirred at 80 °C and 700 rpm for 90 minutes until a clear homogeneous liquid was obtained, which indicated the formation of NADESs. The as-obtained NADESs were as follows: DL-menthol : L-lactic acid (Man : LacA), DL-menthol : *n*-octanoic acid (Man : OctA), DL-menthol : decanoic acid (Man : DecA), DL-menthol : lauric acid (Man : LauA), thymol : *n*-octanoic acid (Thy : OctA), thymol : lauric acid (Thy : LauA), thymol : ethanol (Thy : Eth), thymol : *n*-butanol (Thy : But), thymol : *n*-hexanol (Thy : Hex), Thy : LacA, Thy : Oct and Thy : DecA, as shown in Table S1.†

Synthesis of NADES-$CsPbBr_3$ PNCs

The synthesis processes of NADESs and NADES-$CsPbBr_3$ PNCs are illustrated in Fig. 1. and the NADESs used are listed in Table S2.† In a typical procedure, under vigorous stirring at 50 °C, 0.02 mmol of $PbBr_2$, 100 μL of OA and 75 μL of OAm were dissolved in 1 mL of Thy : Oct, and 0.3 mmol of CsBr were dissolved in 1 mL of Thy : Lac to form Pb- and Cs-precursor solutions. Then, 600 μL of Pb-precursor and 119 μL of Cs-precursor solution (molar ratio of Cs : Pb = 3 : 1) was quickly added to 3 mL of Thy : DecA at the same time under vigorous stirring, and bright blue-green PL emission was observed immediately. After 5 hours, the $CsPbBr_3$ colloidal solution was centrifuged at 10 000 rpm for 10 min to obtain NADES-$CsPbBr_3$ PNCs. Finally, the product was washed and stored in *n*-hexane.

Fabrication of the white LED device

First, the as-synthesized NADES-$CsPbBr_3$ PNCs powders were blended with silicone gel A and B (A : B = 1 : 4) and mixed by stirring to obtain a fine dispersion of NADES-$CsPbBr_3$ PNCs. Then the mixture was vacuumed to discharge air bubbles. A

Published on 11 Oktoba 2022. Downloaded on 26/07/2025 17:39:36.

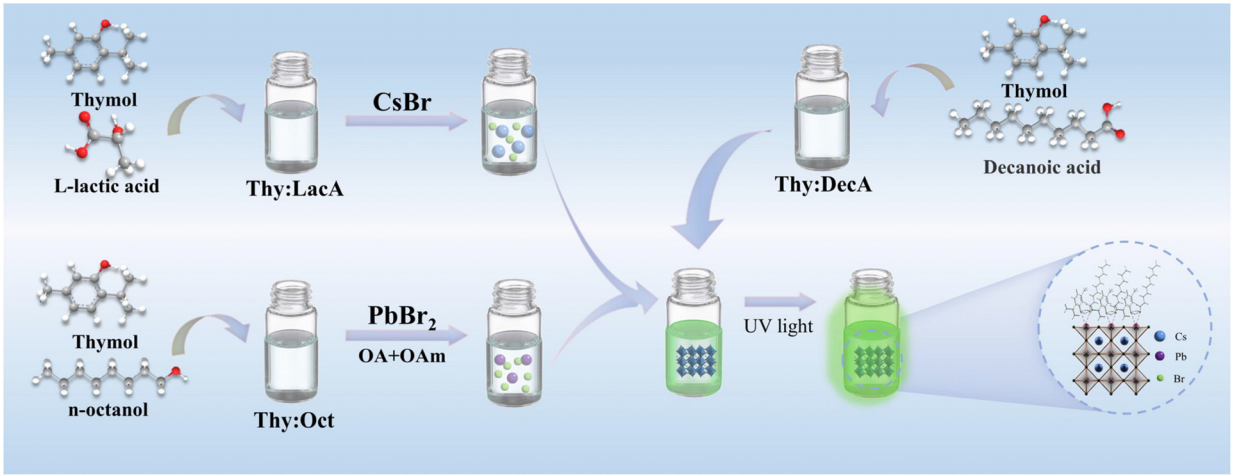

Fig. 1 Schematic illustration of synthetic procedure for NADES-$CsPbBr_3$ PNCs.

WLED device was constructed by combining a 480 nm GaN LED blue chip with the green-emitting NADES-$CsPbBr_3$ PNC glass and commercial red-emitting KSF phosphor.

Results and discussion

Characterization of NADESs

NADESs were formed by the hydrogen bond between HBA and HBD. To prove the formation of Thy : Oct, the FTIR and ^{1}H NMR characterizations of Thy : Oct and their constituents were performed, as shown in Fig. 2. From the FTIR spectra of Thy : Oct and its constituents (Fig. 2a), the broad absorption bands associated with the stretching vibrations of O–H groups were observed in the range 3100–3400 cm^{-1}. Compared with the O–H stretching bands of thymol and octanol respectively located at 3231.40 cm^{-1} and 3317.54 cm^{-1}, the O–H stretching band of Thy : Oct, located at 3342.30 cm^{-1}, was shifted to a higher wavenumber. This result could be regarded as the contribution of the hydrogen bond formation between HBA and HBD, which indicated the formation of Thy : Oct. The ^{1}H NMR spectra of Thy : Oct and its constituents are presented in Fig. 2b. The characteristic H resonance peaks of thymol and octanol can be observed in spectrum of Thy : Oct. Furthermore, the peaks of the –OH of thymol from δ = 4.78 to δ = 6.79 and the –OH group of octanol from δ = 3.74 to δ = 2.88 can be observed. The chemical shift value changes because the formation of hydrogen bonds changes the electron density around the hydrogen nucleus, verifying the formation of Thy : Oct. Similarly, as shown in Fig. S1 and S2,† the formation of Thy : LacA and Thy : DecA can also be proved by FT-IR and ^{1}H NMR.[39,40]

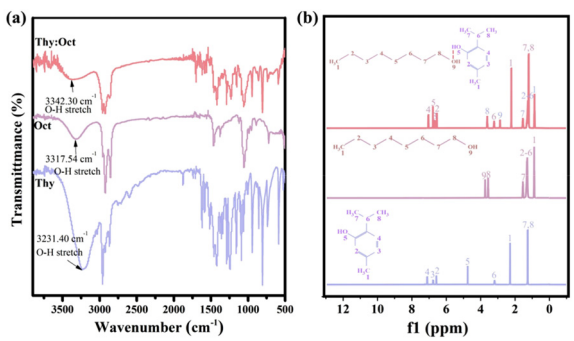

Fig. 2 (a) The FT-IR spectra of thymol, *n*-octanol and Thy : Oct; (b) ^{1}H NMR spectra of thymol, *n*-octanol and Thy : Oct.

The polarity of the NADESs can be evaluated based on the solvatochromic method. Nile red solvatochromic dyes comprise one of the most widely used probes that has been extensively employed to measure the polarity of NADESs.[41] The solvatochromic parameter E_{NR} can be calculated using the following equation:

$$E_{NR} = 28591/\lambda_{max}$$

where E_{NR} is in kcal mol^{-1} and λ_{max} is the wavelength of the maximum absorption of the probe in the NADESs. High E_{NR} values correspond to lower polarity and low E_{NR} values correspond to higher polarity of NADESs. The absorbance spectra of Nile red dissolved in Thy : LacA, Thy : Oct and Thy : DecA is shown in Fig. S3.† The λ_{max} values were located at 592 nm, 566 nm and 563 nm respectively. The polarity values of Thy : LacA, Thy : Oct and Thy : DecA as calculated by E_{NR} scales were 48.3 kcal mol^{-1}, 50.5 kcal mol^{-1} and 50.7 kcal mol^{-1} respectively.

Characterization of NADES-$CsPbBr_3$ PNCs

The phase of NDES-$CsPbBr_3$ NCs were conducted *via* X-ray diffraction (XRD) (Fig. 3a). The diffraction peaks of NADES-$CsPbBr_3$ PNCs and typical $CsPbBr_3$ PNCs were well coincident with a monoclinic phase of $CsPbBr_3$ (PDF card no. 00-018-0364). The diffraction peaks located at 2θ = 15.1°, 21.5°, 30.7°, 34.2°, 37.6° and 43.7° can be assigned to (001), (110), (200), (210), (211) and (202) crystal planes, respectively. Furthermore, compared with the typical LARP-synthesized $CsPbBr_3$ PNCs, NADES-$CsPbBr_3$ PNCs exhibited higher and sharper peaks indicating NADES-$CsPbBr_3$ PNCs have better

 This journal is © The Royal Society of Chemistry 2022

Published on 11 Oktoba 2022. Downloaded on 26/07/2025 17:39:36.

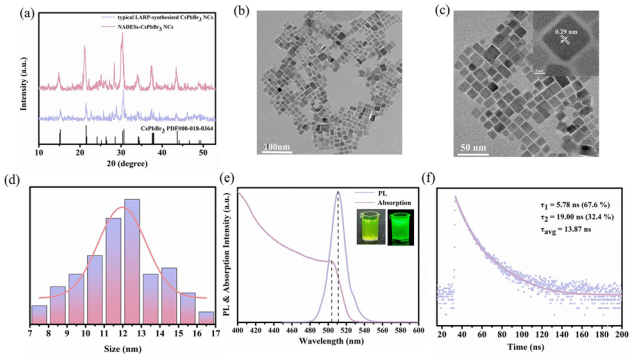

Fig. 3 (a) The XRD patterns of $CsPbBr_3$ PNCs synthesized by two methods; (b and c) TEM images of NADES-$CsPbBr_3$ PNCs. Inset in (c) shows the corresponding HRTEM image; (d) size distribution of NADES-$CsPbBr_3$ PNCs; (e) absorption and PL spectra of NADES-$CsPbBr_3$ PNCs. Inset in (e) shows the photograph of NADES-$CsPbBr_3$ PNCs under daylight (left) and under UV light (right); (f) the decay curve of NADES-$CsPbBr_3$ PNCs.

crystalline quality. The transmission electron microscopy (TEM) graph of NADES-$CsPbBr_3$ PNCs indicated that NADES-$CsPbBr_3$ PNCs possess a cubic shape and is well dispersed (Fig. 3b and c). Moreover, the high-resolution TEM image (inset of Fig. 3c) revealed a highly ordered crystalline lattice and the lattice spacing was calculated to be 0.29 nm, which corresponds to the (200) lattice space of monoclinic $CsPbBr_3$ PNCs. The size ranged from 7 to 18 nm and the average widths were around 11.8 nm as illustrated in Fig. 3d.

Optical properties of the as-synthesized NADES-$CsPbBr_3$ PNCs were also studied. The UV-vis absorption and PL emission spectra of NADES-$CsPbBr_3$ PNCs are presented in Fig. 3e. The UV-vis absorption spectra showed an obvious shoulder peak at about 504 nm. Meanwhile, a single strong PL peak appeared at around 511 nm with a narrow FWHM of ~18.8 nm. As shown in Fig. S4,† the as-synthesized NADES-$CsPbBr_3$ NCs exhibited a high PLQY value of ~96.8%. The inset of Fig. 3e shows a NADES-$CsPbBr_3$ PNC yellow-green solution under daylight, and bright green light emission under UV light. Furthermore, the time-resolved PL measurements were carried out to verify the exciton recombination dynamics, as shown in Fig. 3f. The PL decay could be well fitted by a biexponential function,[15]

$$A(t) = A_1 \exp\left(\frac{-t}{\tau_1}\right) + A_2 \exp\left(\frac{-t}{\tau_2}\right)$$

where A, A_1, and A_2 are constants and τ_1 and τ_2 are two biexponential lifetimes with amplitudes A_1 and A_2, respectively. The average lifetime (τ_{ave}) can be calculated as

$$\tau_{ave} = \frac{A_1\tau_1^2 + A_2\tau_2^2}{A_1\tau_1 + A_2\tau_2}$$

The obtained NADES-$CsPbBr_3$ PNCs exhibit two lifetimes (τ): τ_1 of 5.78 ns accounting for 67.6%, and τ_2 of 19.00 ns accounting for 32.4%, respectively. The short decay time (τ_1) originated from excitonic radiative recombination, while the long decay time originated from a longer charge trapping/detrapping process.[42] The longer τ_2 of NADES-$CsPbBr_3$ PNCs is consistent with its higher surface defects, while the smaller proportion of τ_2 indicates the low defect density of the synthesized NADES-$CsPbBr_3$ PNCs. However, this may need further spectroscopic study.

The selection of NADESs

The synthesis of $CsPbBr_3$ PNCs by the supersaturation recrystallization method was achieved through dissolving the precursors in a good solvent, and then transferring them into a poor solvent (antisolvents) to form a supersaturated solution and precipitate crystals. Therefore, the solubility of precursors in the related solvents plays an important role in this method. The solubility of CsBr and $PbBr_2$ in 13 kinds of NADESs was investigated and is summarized in Table S3.† As can be seen, CsBr could dissolve in Thy : LacA, and $PbBr_2$ could dissolve in four NADESs, comprising Thy : Oct, Thy : But, Thy : Hex and Thy : Oct. To further obtain the best dissolve solvents of $PbBr_2$, four different schemes (Table 1) were designed to synthesize NADES-$CsPbBr_3$ PNCs and the PL spectra of the products were investigated (Fig. 4a). As shown in Fig. 4a, the NADES-$CsPbBr_3$ PNCs synthesized *via* the TLTO scheme exhibited the best optical properties. Hence, Thy : LacA and Thy : Oct were used as the dissolving solvents for CsBr and $PbBr_2$, respectively. Furthermore, the optimal NADES to be used as an antisolvent was also evaluated. It can be seen from Fig. 4b and Table S4† that the NADES-$CsPbBr_3$ PNC synthesized using Thy : DecA as an antisolvent showed the strongest PL intensity. Therefore, Thy : DecA was selected as the antisolvent in this experiment.

Effect of the concentration of Cs- and Pb-precursor solutions

As the structural disintegration of PNCs is likely to occur in a good solvent, it is necessary to use highly concentrated precursor solutions to reduce the amount of good solvent required in the LARP method. To investigate the influence of the concentration of Cs- and Pb-precursor solutions on the luminescence intensity of NADES-$CsPbBr_3$ PNCs in this method, a series of experiments were studied using various concentrations of Cs- and Pb-precursor solutions (Table S5 and S6†). Fig. 4c and d showed that the luminescence intensity of NADES-$CsPbBr_3$ PNCs was increased with the increase in the concentration of Cs- and Pb-precursor solutions, and the highest intensity was

Table 1 Different combination schemes used to synthesize NADES-$CsPbBr_3$ PNCs

Name	CsBr	$PbBr_2$	Antisolvent
TLTE	Thy : LacA ($0.3\ mol{\cdot}L^{-1}$)	Thy : Eth ($0.02\ mol{\cdot}L^{-1}$)	Thy : DecA (3 mL)
TLTB	Thy : LacA ($0.3\ mol{\cdot}L^{-1}$)	Thy : But ($0.02\ mol{\cdot}L^{-1}$)	Thy : DecA (3 mL)
TLTH	Thy : LacA ($0.3\ mol{\cdot}L^{-1}$)	Thy : Hex ($0.02\ mol{\cdot}L^{-1}$)	Thy : DecA (3 mL)
TLTO	Thy : LacA ($0.3\ mol{\cdot}L^{-1}$)	Thy : Oct ($0.02\ mol{\cdot}L^{-1}$)	Thy : DecA (3 mL)

Published on 11 Oktoba 2022. Downloaded on 26/07/2025 17:39:36.

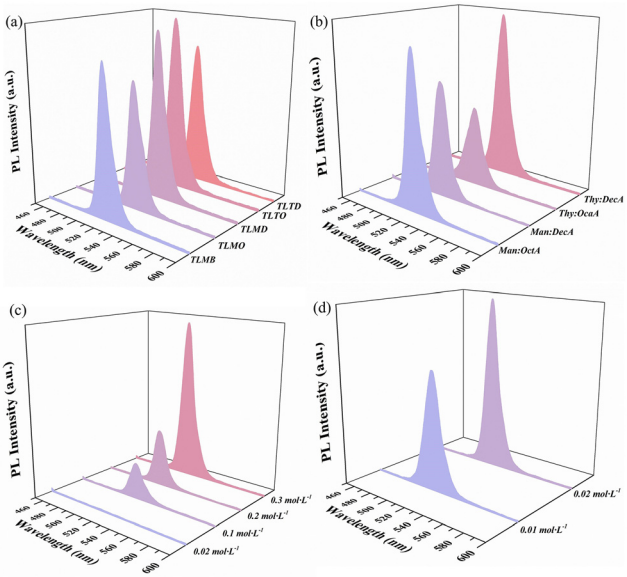

Fig. 4 (a) PL spectra of NADES-$CsPbBr_3$ PNCs synthesized by different schemes; (b) PL spectra of NADES-$CsPbBr_3$ PNCs synthesized by different antisolvents; (c) PL spectra of NADES-$CsPbBr_3$ PNCs synthesized by different concentration of Cs-precursor; (d) PL spectra of NADES-$CsPbBr_3$ PNCs synthesized by different concentrations of Pb-precursor.

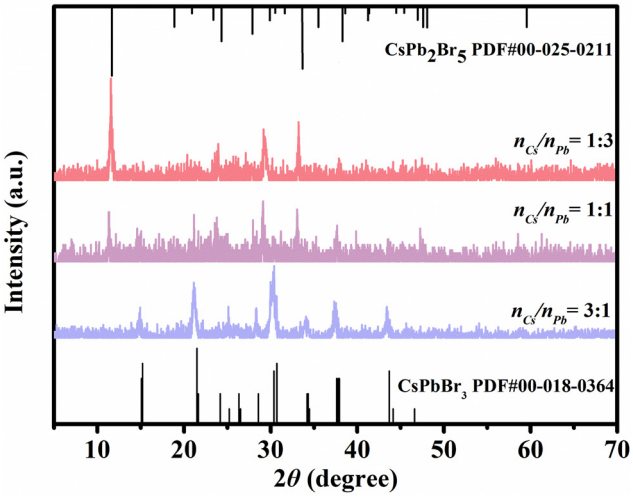

Fig. 5 XRD patterns of PNCs synthesized with different molar ratios of CsBr and $PbBr_2$.

obtained at up to 0.3 mol L^{-1} Cs-precursor solutions and 0.02 mol L^{-1} Pb-precursor solutions, respectively.

Optimum molar ratios of Pb- and Cs-precursor

The molar ratios of Pb- and Cs-precursor (n_{Cs}/n_{Pb}) significantly affect the phase transformation of PNCs. Fig. 5 presents the XRD patterns of PNCs with different n_{Cs}/n_{Pb} ratios (1 : 3, 1 : 1 and 3 : 1). The phase of the PNCs gradually changed from $CsPb_2Br_5$ to $CsPbBr_3$ PNCs with the increase in n_{Cs}/n_{Pb}. Different from the pure phase of $CsPbBr_3$ PNCs formed in the typical method, mixed phases of $CsPb_2Br_5$ and $CsPbBr_3$ PNCs were obtained with n_{Cs}/n_{Pb} = 1 : 1 in this method. This was probably caused by the strong coordination between Cs^+ and Thy : LacA. When n_{Cs}/n_{Pb} reached 3 : 1, the pure phase of $CsPbBr_3$ PNCs was obtained, for which the XRD pattern was assigned to three dimensional $CsPbBr_3$ (PDF card no.00-018-0364). Hence, n_{Cs}/n_{Pb} = 3 : 1 was selected in our experiment.

Stability of NADES-$CsPbBr_3$ PNCs

To avoid the reduction of the applied device performance by the residual organic ligands, purification processes of PNCs are necessary. Unfortunately, in the typical LARP-synthesized $CsPbBr_3$ PNCs, the shift of the UV-vis peak and the PL quenching phenomenon were observed because of severe aggregation of PNCs due to insufficient surface ligands after only two washing cycles (Fig. S5†). According to previous reports,[43,44] the OA/OAm ligands were easily washed off because of their proton exchange and weak coordination ability with PNCs. In contrast, NADES-$CsPbBr_3$ PNCs exhibited much higher stability during purification processes. NADESs have a stronger coordination ability with PNCs and act as better surface ligands, which prevents the aggregation of PNCs. As shown in Fig. 6a and b, the UV-vis absorption and PL spectra of NADES-$CsPbBr_3$ PNCs barely changed after five cycles of the same washing processes.

The storage, light, thermal and water stability of NADES-$CsPbBr_3$ PNCs were further determined. The storage stability of the NADES-$CsPbBr_3$ PNCs was evaluated in ambient conditions and the results are shown in Fig. 6c. It can be seen that the PL emission intensity could preserve 82.9% retention after 70 days. As shown in Fig. 6d, the typical LARP-synthesized $CsPbBr_3$ PNCs only kept 0.6% of the initial PL intensity under irradiation with a UV lamp after 9 h, while 47.6% of the initial PL intensity of NADES-$CsPbBr_3$ PNCs was still reserved. In addition, as exhibited in Fig. 6e, the typical LARP-synthesized $CsPbBr_3$ PNCs kept 0.7% of the initial PL intensity after nine heating cycles at 85 °C, while the PL intensity of NADES-$CsPbBr_3$ PNCs could still be maintained at 43.8%. Finally, the water stability of $CsPbBr_3$ PNCs was tested by 2 mL of hexane solution put on the top of 1 mL of water (Fig. 6f). For the typical LARP-synthesized $CsPbBr_3$ PNCs, green fluorescence disappeared completely after 40 h, while the NADES-$CsPbBr_3$ PNCs maintained bright fluorescence. All these results demonstrate that, compared to the typical LARP-synthesized $CsPbBr_3$ PNCs, the stability of NADES-$CsPbBr_3$ PNCs was significantly improved.

Formation mechanism of NADES-$CsPbBr_3$ PNCs

To further understand the formation mechanism of NADES-$CsPbBr_3$ PNCs, the role of NADESs in this method is discussed. On the one hand, NADESs were used as solvents in the LARP method. To measure the dissolving capacity of three NADESs for CsBr and $PbBr_2$, their polarity was evaluated through the Nile red polarity scale. As a result, CsBr can directly dissolved in Thy : LacA of high polarity, and $PbBr_2$ can

This journal is © The Royal Society of Chemistry 2022

Published on 11 Oktoba 2022. Downloaded on 26/07/2025 17:39:36.

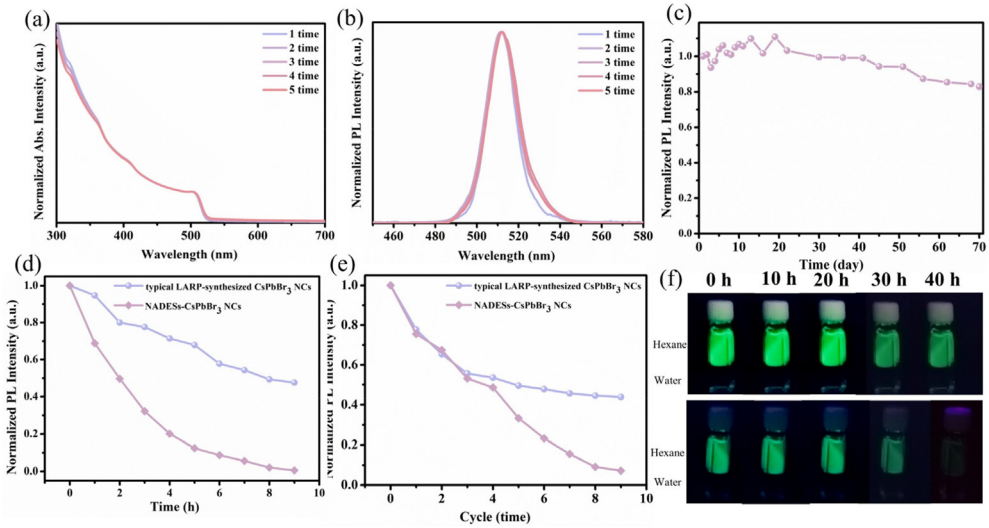

Fig. 6 (a) The UV-vis patterns of NADES-$CsPbBr_3$ NC by different centrifugation times; (b) PL spectra of NADES-$CsPbBr_3$ PNCs by different centrifugation times; (c) time stability of NADES-$CsPbBr_3$ PNCs; (d) light stability of $CsPbBr_3$ PNCs; (e) thermal stability of $CsPbBr_3$ PNCs; (f) water stability of $CsPbBr_3$ PNCs. Above is NADES-$CsPbBr_3$ PNCs; below is typical LARP-synthesized $CsPbBr_3$ PNCs. Upper layer, hexane; bottom layer, water.

dissolve in Thy : Oct of lower polarity with the help of the coordination of OA/OAm. Meanwhile, Thy : DecA of the lowest polarity can be used as an antisolvent, leading to the mixture becoming a supersaturated solution and precipitating crystals to form NADES-$CsPbBr_3$ PNCs. On the other hand, NADESs were also used as surface ligands of $CsPbBr_3$ PNCs. For the synthesis of PNCs, introducing some organic molecules is necessary, which can strongly interact with ions and control crystal growth kinetics to reduce the defect density.[45] To verify the feasibility of using NADESs as surface ligands, the crystal growth kinetics and ^{1}H NMR characterization of NADES-$CsPbBr_3$ PNCs were performed. It can be seen from Fig. S6,† that the fluorescence of NADES-$CsPbBr_3$ PNCs changed from blue to green and the intensity gradually increased with the reaction time and reached the highest value at 5 h. The main reason for the difference from the rapid crystallization of typical synthetic PNCs is that the –COOH and –OH groups of NADESs can strongly coordinate with the Pb of $CsPbBr_3$ PNCs. From the ^{1}H NMR spectra of NADES-$CsPbBr_3$ PNCs OA and OAm (Fig. 7), it can be found that there is no carbon–carbon double bond characteristic hydrogen peak (δ = 5.37) of OA and OAm in NADES-$CsPbBr_3$ PNCs, which indicates that not oleylamine oleate but NADESs can act as surface ligands to effectively passivate PNCs.

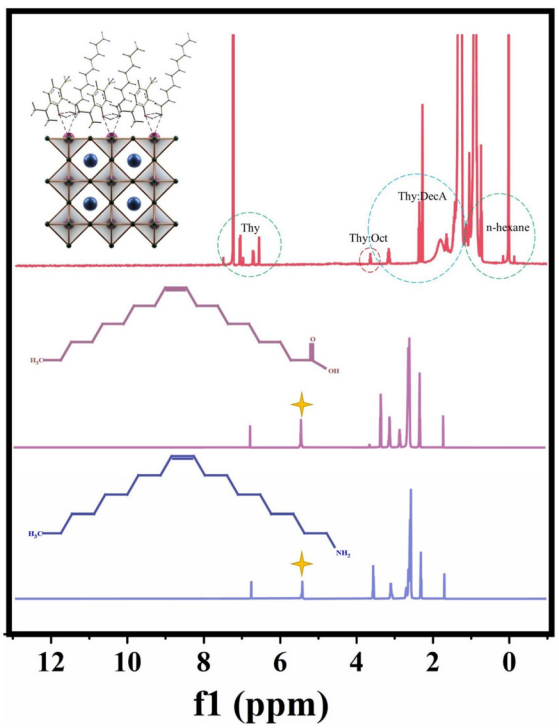

Fig. 7 ^{1}H NMR spectra of NADES-$CsPbBr_3$ PNCs, OA and OAm.

Light-emitting devices

Finally, the obtained NADES-$CsPbBr_3$ NCs with a bright pure green emission were applied for fabricating a WLED lamp based on a commercially available 460 nm GaN LED blue chip (the inset in Fig. 8a). Fig. 8a shows the typical electroluminescence (EL) spectra of the WLED at a driving current of 20 mA. To further investigate the potential applications of NADES-$CsPbBr_3$ NCs, we measured the luminous efficiency of the WLED driven by different currents, as shown in Fig. S7.† The highest power efficiency reached 55.61 Lm W^{-1} under a 20 mA current. The color coordinates of the sample were labeled as a red dot with a corresponding color coordinate of (0.3164, 0.3242) in the Commission International de l'Eclairage (CIE) chromaticity diagram (Fig. 8b). Therefore, the obtained NADES-$CsPbBr_3$ PNCs reveal their potential commercial application in the light field.

Published on 11 Oktoba 2022. Downloaded on 26/07/2025 17:39:36.

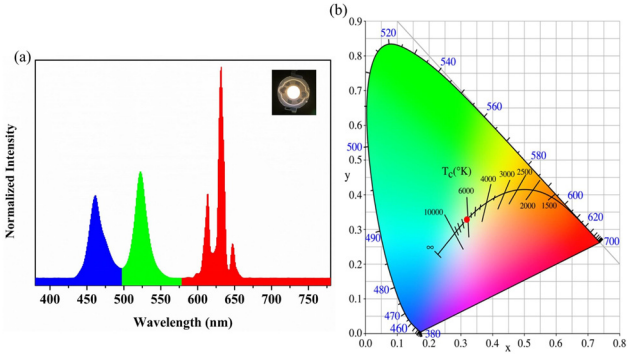

Fig. 8 (a) PL emission spectrum. The inset shows the photograph of device in open states; (b) CIE coordinates of NADES-$CsPbBr_3$ PNCs in CIE space.

Conclusions

In summary, the work focuses on designing a toxic organic solvent-free approach to the synthesis of $CsPbBr_3$ PNCs based on NADESs, for meeting the environment-friendly requirements to achieve the preparation of high-performance LED chips. The as-prepared NADES-$CsPbBr_3$ PNCs exhibit a high PLQY of ~96.8%, a narrow FWHM of ~18.8 nm and excellent stability. NADESs can not only use function as solvents, but also serve as a surface ligand to effectively reduce defects for the green synthesis of highly stable, bright-luminous NADES-$CsPbBr_3$ PNCs. Besides, a WLED lamp was fabricated to verify its practical application. Compared to the traditional LARP method, our method is simple and eco-friendly, which is desirable for the large-scale production of perovskite, and opens a new synthesis pathway to green exploitation of perovskite materials.

Author contributions

Heng Lu: conceptualization, methodology, investigation, writing – original draft, formal analysis. Xiaohong Tan: methodology and resources. Guobin Huang: data curation, writing – review and editing. Shaoru Wu: investigation. Yanmei Zhou: visualization and supervision. Junying Zhang: investigation. Qiaowen Zheng: investigation and editing. Tianju Chen: visualization. Feiming Li: editing. Zhixiong Cai: editing. Jingbin Zeng: methodology, investigation and editing. Maosheng Zhang: supervision, project administration, funding acquisition.

Conflicts of interest

The authors declare that they have no known competing financial interests or personal relationships that could have appeared to influence the work reported in this paper.

Acknowledgements

This work was supported by the National Natural Science Foundation of China (nos 21904055 and 22004055), Natural Science Foundation of Fujian Province, China (nos 2021H6033, 2020J05165 and 2020J05164), Science and Technology Projects of the Education Department, Fujian Province of China (no. JK2017032), and the Natural Science Foundation of Zhangzhou City, China (no. ZZ2019J02).

References

1 G. Huang, Y. Zhou, F. Li, X. Tan, Z. Cai, D. Luo, T. Chen and M. Zhang, *Sens. Actuators, B*, 2021, **347**, 130618.
2 J. Song, T. Fang, J. Li, L. Xu, F. Zhang, B. Han, Q. Shan and H. Zeng, *Adv. Mater.*, 2018, **30**, 1805409.
3 G. Xing, N. Mathews, S. S. Lim, N. Yantara, X. Liu, D. Sabba, M. Grätzel, S. Mhaisalkar and T. C. Sum, *Nat. Mater.*, 2014, **13**, 476–480.
4 Y. Zhou, S. Wu, G. Huang, J. Zeng, B. E. Meteku, X. Tan, H. Lu, F. Li, Z. Cai, X. Wang and M. Zhang, *J. Alloys Compd.*, 2022, **918**, 165565.
5 K. Lin, J. Xing, L. N. Quan, F. P. G. de Arquer, X. Gong, J. Lu, L. Xie, W. Zhao, D. Zhang, C. Yan, W. Li, X. Liu, Y. Lu, J. Kirman, E. H. Sargent, Q. Xiong and Z. Wei, *Nature*, 2018, **562**, 245–248.
6 J. Ali, Y. Li, P. Gao, T. Hao, J. Song, Q. Zhang, L. Zhu, J. Wang, W. Feng, H. Hu and F. Liu, *Nanoscale*, 2020, **12**, 5719–5745.
7 K. Fu, C. T. Nelson, M. C. Scott, A. Minor, N. Mathews and L. H. Wong, *Nanoscale*, 2016, **8**, 4181–4193.
8 S. Ghimire and C. Klinke, *Nanoscale*, 2021, **13**, 12394–12422.
9 L. Lei, Q. Dong, K. Gundogdu and F. So, *Adv. Funct. Mater.*, 2021, **31**, 2010144.
10 M. Palabathuni, S. Akhil, R. Singh and N. Mishra, *ACS Appl. Nano Mater.*, 2022, **5**, 10097–10117.
11 S. Akhil, V. G. V. Dutt, R. Singh and N. Mishra, *J. Phys. Chem. C*, 2021, **125**, 22133–22141.
12 S. Akhil, V. G. V. Dutt and N. Mishra, *Nanoscale Adv.*, 2021, **3**, 2547–2553.
13 L. Protesescu, S. Yakunin, M. I. Bodnarchuk, F. Krieg, R. Caputo, C. H. Hendon, R. X. Yang, A. Walsh and M. V. Kovalenko, *Nano Lett.*, 2015, **15**, 3692–3696.
14 X. Li, Y. Wu, S. Zhang, B. Cai, Y. Gu, J. Song and H. Zeng, *Adv. Funct. Mater.*, 2016, **26**, 2435–2445.
15 F. Zhang, H. Zhong, C. Chen, X.-G. Wu, X. Hu, H. Huang, J. Han, B. Zou and Y. Dong, *ACS Nano*, 2015, **9**, 4533–4542.
16 W. Li, W. Deng, X. Fan, F. Chun, M. Xie, C. Luo, S. Yang, H. Osman, C. Liu, X. Zheng and W. Yang, *Ceram. Int.*, 2018, **44**, 18123–18128.
17 T. Chen, Y. Xu, Z. Xie, W. Jiang, L. Wang and W. Jiang, *Nanoscale*, 2020, **12**, 9569–9580.
18 H. Luo, Y. Huang, H. Liu, B. Zhang and J. Song, *Chem. Eng. J.*, 2022, **430**, 132790.

This journal is © The Royal Society of Chemistry 2022

Published on 11 Oktoba 2022. Downloaded on 26/07/2025 17:39:36.

19 M. T. Clough, K. Geyer, P. A. Hunt, S. Son, U. Vagt and T. Welton, *Green Chem.*, 2015, **17**, 231–243.
20 L. Yang, H. Wang, Y.-G. Zu, C. Zhao, L. Zhang, X. Chen and Z. Zhang, *Chem. Eng. J.*, 2011, **172**, 705–712.
21 Y. Tan, Y. Zou, L. Wu, Q. Huang, D. Yang, M. Chen, M. Ban, C. Wu, T. Wu, S. Bai, T. Song, Q. Zhang and B. Sun, *ACS Appl. Mater. Interfaces*, 2018, **10**, 3784–3792.
22 S. Akhil, V. G. V. Dutt and N. Mishra, *Nanoscale*, 2021, **13**, 13142–13151.
23 S. Akhil, V. G. V. Dutt, R. Singh and N. Mishra, *J. Phys. Chem. C*, 2022, **126**, 10742–10751.
24 S. Akhil, V. G. V. Dutt and N. Mishra, *ChemNanoMat*, 2021, **7**, 342–353.
25 S. Akhil, V. G. V. Dutt and N. Mishra, *Chem. – Eur. J.*, 2020, **26**, 17195–17202.
26 A. P. Abbott, G. Capper, D. L. Davies, R. K. Rasheed and V. Tambyrajah, *Chem. Commun.*, 2003, **1**, 70–71.
27 Y. Fan, H. Wu, D. Cai, T. Yang and L. Yang, *Sep. Purif. Technol.*, 2020, **250**, 117211.
28 A. P. Abbott, D. Boothby, G. Capper, D. L. Davies and R. K. Rasheed, *J. Am. Chem. Soc.*, 2004, **126**, 9142–9147.
29 A. Paiva, R. Craveiro, I. Aroso, M. Martins, R. L. Reis and A. R. C. Duarte, *ACS Sustainable Chem. Eng.*, 2014, **2**, 1063–1071.
30 Y. Dai, J. van Spronsen, G. J. Witkamp, R. Verpoorte and Y. H. Choi, *Anal. Chim. Acta*, 2013, **766**, 61–68.
31 Y. Ma, Y. Li, S. Ali, P. Li, W. Zhang, M. C. R. Rauch, S. J. P. Willot, D. Ribitsch, Y. H. Choi, M. Alcalde, F. Hollmann and Y. Wang, *ChemCatChem*, 2020, **12**, 989–994.
32 T.-X. Yang, L.-Q. Zhao, J. Wang, G.-L. Song, H.-M. Liu, H. Cheng and Z. Yang, *ACS Sustainable Chem. Eng.*, 2017, **5**, 5713–5722.
33 W. Liu, K. Zhang, J. Chen and J. Yu, *J. Mol. Liq.*, 2018, **260**, 173–179.
34 Á. Santana-Mayor, A. V. Herrera-Herrera, R. Rodríguez-Ramos, B. Socas-Rodríguez and M. Á. Rodríguez-Delgado, *ACS Sustainable Chem. Eng.*, 2021, **9**, 2161–2170.
35 D. Fuchs, B. C. Bayer, T. Gupta, G. L. Szabo, R. A. Wilhelm, D. Eder, J. C. Meyer, S. Steiner and B. Gollas, *ACS Appl. Mater. Interfaces*, 2020, **12**, 40937–40948.
36 F. J. V. Gomez, M. Espino, M. de los Angeles Fernandez, J. Raba and M. F. Silva, *Anal. Chim. Acta*, 2016, **936**, 91–96.
37 Q. Hu, H. Yu, S. Gong, Q. Han and W. Wu, *J. Mater. Chem. C*, 2022, **10**, 6002–6008.
38 M. Wang, F. Qiao and H. Yan, *Green Chem.*, 2021, **23**, 5179–5188.
39 J. Yue, Z. Zhu, J. Yi, H. Li, B. Chen and J. Rao, *Food Chem.*, 2022, **376**, 131943.
40 K. Zhu, Q. Wei, H. Li and X. Ren, *ACS Sustainable Chem. Eng.*, 2022, **10**, 2125–2135.
41 A. K. Dwamena and D. E. Raynie, *J. Chem. Eng. Data*, 2020, **65**, 640–646.
42 M. T. Hoang, N. D. Pham, Y. Yang, V. T. Tiong, C. Zhang, K. Gui, H. Chen, J. Chang, J. Wang, D. Golberg, J. Bell and H. Wang, *Green Chem.*, 2020, **22**, 3433–3440.
43 Y. Liu, D. Li, L. Zhang, Y. Chen, C. Geng, S. Shi, Z. Zhang, W. Bi and S. Xu, *Chem. Mater.*, 2020, **32**, 1904–1913.
44 Q. Zhong, M. Cao, Y. Xu, P. Li, Y. Zhang, H. Hu, D. Yang, Y. Xu, L. Wang, Y. Li, X. Zhang and Q. Zhang, *Nano Lett.*, 2019, **19**, 4151–4157.
45 Y. Liu, X. Zheng, Y. Fang, Y. Zhou, Z. Ni, X. Xiao, S. Chen and J. Huang, *Nat. Commun.*, 2021, **12**, 1686.